J. Phys. Soc. Jpn.
Downloaded from journals.jps.jp by Uppsala Universitetsbibliotek on 05/25/18

Journal of The Physical Society of Japan
Vol. 62, No. 2, February, 1993, pp. 811–817

Valence States of Rare-Earth Ions in $RERuSn_3$ (RE=La, Ce, Pr, Nd, Sm) and Related Compounds Studied by Core-Level Photoemission Spectroscopy

Hiroyoshi ISHII, Takaaki HANYU, Tadashi FUKUHARA,†
Isao SAKAMOTO,†† Hideyuki SATO and Shigeo YAMAGUCHI

Department of Physics, Faculty of Science, Tokyo Metropolitan University, Minami Ohsawa 1-1, Hachioji-shi, Tokyo 192-03
†Toyama Prefectural University, Kosugi-mati, Toyama 939-03
††Nagoya Institute of Technology, Nagoya-shi, Aichi 466

(Received September 8, 1992)

We have measured the 3*d* and 4*d* core-level X-ray photoelectron spectra of rare earths in $RERuSn_3$ (RE=La, Ce, Pr, Nd and Sm) and related rare-earth compounds. The Ce 3*d* spectra of $CeRuSn_x$ (x=2.85, 3.0 and 3.15) show the common features observed in other cerium compounds. In the spectra, f^0 structures cannot be apparently distinguished from other prominent structures f^1 and f^2 peaks, and broad structures are observed at the high binding energy side of the f^1 peak. For $SmRuSn_3$, both Sm 3*d* and 4*d* spectra show strong Sm^{2+} components and the Sm valency is estimated to be 2.95 ± 0.02.

[rare earth, $CeRuSn_3$, $SmRuSn_3$, heavy fermion, mixed valence, valency, XPS, core level]

§1. Introduction

Rare-earth compounds have been investigated by various transport and spectroscopic methods because of their unusual physical properties.[1-6] Spectroscopic properties of these materials have directly given the information about the 4*f* electronic states. In particular, the valency of rare earths has been estimated in detail. The difference in valency between the spectroscopic and transport investigations has been pointed out.[1,2,5,6]

$RERuSn_3$ (RE=La, Ce, Pr, Nd and Sm) samples are interesting materials;[7] $CeRuSn_3$ is known as a heavy fermion system, and $SmRuSn_3$ is thought to be a mixed valence system. In this paper, we will report about the occupancy of 4*f* electrons in the heavy fermion system and the other reference rare-earth compounds by the core-level photoemission spectroscopy. The X-ray photoelectron spectrum (XPS) of a core level of a rare earth has several peaks at the different energy positions due to the different final states of photoexcitation. The intensities of these peaks can provide the information about the number of 4*f* electrons and the hybridization between the 4*f* electrons and the conduction electrons in a rare-earth compound. The study by the core-level photoemission spectroscopy is more useful for estimating the valency of a rare earth than that by the valence band photoemission spectroscopy.

In this experiment, the Sm valency of $SmRuSn_3$ was investigated to decide directly whether this compound is a mixed valence system. For a metallic samarium compound, however, the 4*f* electronic state in the surface layer has been considered to be largely different from that in the bulk.[8-11] It is necessary to consider the contribution of the surface state to the core-level spectrum. We measured the Sm 3*d* and 4*d* XPS spectra of $SmRuSn_3$ and some materials with trivalent samarium ions; the Sm 4*d* XPS spectrum is more sensitive to the 4*f* electronic state in the bulk than the Sm 3*d* XPS spectrum. The intensities of Sm^{2+} components in the core-level spectra of $SmRuSn_3$ were compared with those of trivalent samarium compounds.

J. Phys. Soc. Jpn.
Downloaded from journals.jps.jp by Uppsala Universitetsbibliotek on 05/25/18

§2. Experimental

The polycrystalline $RERuSn_3$, $CeRuSn_x$, $Sm_3Rh_4Sn_{13}$, $SmSn_3$, $SmAl_2$, $SmGa_2$ and $SmPd_3$ samples were prepared by arc-melting appropriate amounts of pure elements. The powder of SmB_6 and the chunk of SmSb were melted in crucibles. Sm_2CuO_4 sample was obtained by sintering the mixture of Sm_2O_3 and CuO powders. The XPS spectra were measured using Al $K\alpha$ ($h\nu=1486.6$ eV) and Mg $K\alpha$ radiations ($h\nu=1253.6$ eV). The kinetic energies of photoelectrons ejected at 45° with respect to the sample surface were analyzed. The overall instrumental resolution was ~ 1.1 eV. The pressure was $\sim 3\times 10^{-10}$ Torr during the measurement. The clean surfaces of the samples were prepared by scraping with a diamond file. The cleanness of the surface was checked by the signal from the O 1*s* level. No O 1*s* signal could be detected except for Sm_2CuO_4. The XPS spectra of $CeRuSn_x$ were measured at 100 K and those of the other samples were done at room temperature.

§3. Results and Discussion

3.1 Rare-earth 3d spectra of RERuSn₃

Figure 1 shows the rare-earth 3*d* XPS spectra of $RERuSn_3$ aligned with the nominal 4*f* counts. All these spectra exhibit features similar to those in the rare-earth compounds with non-integral number of 4*f* electrons.[1,2] In general, the Ce 3*d* spectrum shows the three structures f^0, f^1 and f^2 peaks corresponding to the final state configurations $3d^94f^0$, $3d^94f^1$ and $3d^94f^2$, respectively; the f^0 peak is too weak to detect apparently.[2,3,5] In this study, the f^0 peak is also indistinguishable from other structures as can be seen in Fig. 1: the f^0 peak should appear at the high binding energy side of the f^1 peak in the Ce $3d_{3/2}$ peak. According to the analyses of Gunnarsson and Schönhammer[5] and Fuggle *et al.*,[2] the weight of the f^0 peak is related to the number of 4*f* electrons in the ground state. For $CeRuSn_3$, the weak f^0 structure indicates that the number of 4*f* electrons is nearly equal to one in the ground state. On the other hand, the f^{n+1} shoulder structure is sensitive to the strength of the hybridization between the 4*f* electrons and the conduction electrons. To obtain the information about the hybridization, we estimated the area ratios of the f^{n+1} shoulders to the f^n peaks from these rare-earth 3*d* spectra by assuming that the f^n peaks are fitted by a convolution of a Lorentzian and a Gaussian. The ratios are dependent on the element of rare earth in $RERuSn_3$. The ratios decrease in proportion to the nominal 4*f* counts; 0.12, 0.08, 0.06 and 0.06 with an experimental accuracy of 0.02 for RE=La, Ce, Pr and Nd, respectively. Except for $LaRuSn_3$, these ratios are almost equal to each other. In the ground state, the 4*f* count is zero in a La-compound. Accordingly, the final state configurations can be considered to be two states $3d^94f^0$ and $3d^94f^1$. It is considered that the contribution

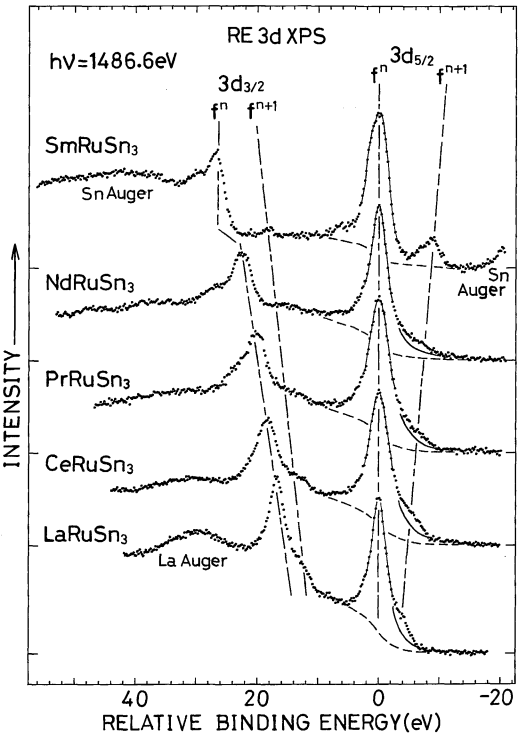

Fig. 1. XPS spectra of the RE 3*d* core levels of $RERuSn_3$ (RE=La, Ce, Pr, Nd and Sm). The zero of the binding energy is taken at the RE $3d_{5/2}$ peak positions. The intensities are normalized to the heights of the RE $3d_{5/2}$ peaks. The structures excited by Al $K\alpha_{3,4}$ satellite were removed from the raw spectra using the intensity ratio of $K\alpha_{3,4}$ to $K\alpha_{1,2}$ radiations. The dashed lines and the solid lines at the relative binding energies $-4\sim-10$ eV indicate the inelastic backgrounds and the calculated tails of the f^n peaks, respectively.

J. Phys. Soc. Jpn.
Downloaded from journals.jps.jp by Uppsala Universitetsbibliotek on 05/25/18

of the ligand site to the f^1 peak is large compared with that for the other rare-earth compounds, $CeRuSn_3$, $PrRuSn_3$ and $NdRuSn_3$.

For $SmRuSn_3$, the structure corresponding to the final state $3d^9 4f^{n+1}$ ($n=5$) appears strongly. Many samarium compounds have been investigated spectroscopically.[1,4,8-11] Considering these results, this peak is attributed to the presence of the divalent state in the ground state. In the latter section, the divalent state will be discussed in detail.

3.2 *Dependence of the Ce 3d spectra of CeRuSn$_x$ on Sn content*

The transport and magnetic properties of $CeRuSn_x$ have showed the dependence on Sn content x.[7] In the temperature dependence of the resistivity and the magnetic susceptibility, the abrupt change took place in the narrow range of composition deviated from the stoichiometric ratio ($x=3.0$). The changes of the properties with x may be dependent on the density of states at the Fermi level. It is interesting to investigate spectroscopically the transient behaviors of $CeRuSn_x$.

The Ce 3*d* XPS spectra of $CeRuSn_x$ are shown in Fig. 2. All spectra show features similar to those of $CeRuSn_3$. The change of the spectral shape with Sn content x was not detected. In this region of the Sn content, the electronic states in $CeRuSn_x$ can be considered to be almost the same in the view of the core-level photoemission spectroscopy.

3.3 *Broad structures appeared in the high binding energy region of the 3d$_{3/2}$ peaks*

As can be seen in Fig. 1, the broad structures appear in the high binding energy region of the RE $3d_{3/2}$ peaks. These structures are complicated owing to the existence of many decay processes filling the core hole during photoexcitation. In various interpretations, the plasmon satellite has been considered to be reliable. Recently, the detailed experimental results about these structures were reported for CeSb and LaSb,[12] and the theoretical analysis was carried out on the basis of their data by Takeshige *et al.*[13] They have stated that the *p-d* screening process contributes to the broad structures. In this study, similar structures were observed in the 3*d* XPS spectra of the

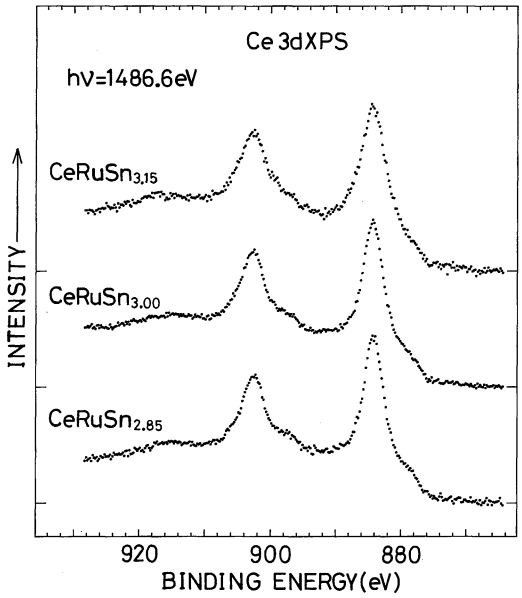

Fig. 2. Ce 3*d* XPS spectra of $CeRuSn_x$ ($x=2.85$, 3.0 and 3.15).

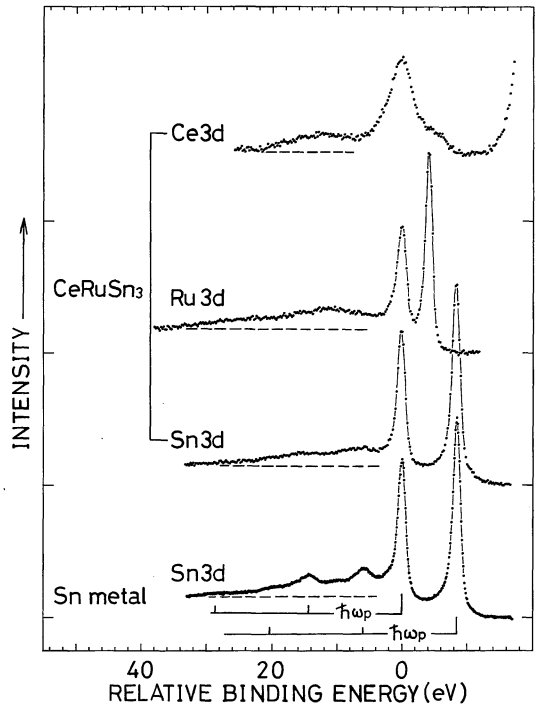

Fig. 3. Ce 3*d*, Ru 3*d* and Sn 3*d* XPS spectra of $CeRuSn_3$ and the Sn 3*d* XPS spectrum of Sn metal. The Ce 3*d* XPS spectrum was measured at Al $K\alpha$ excitation, and the Sn 3*d* and Ru 3*d* XPS spectra at Mg $K\alpha$ excitation. The zero of the binding energy is taken at the $3d_{3/2}$ peak positions.

J. Phys. Soc. Jpn.
Downloaded from journals.jps.jp by Uppsala Universitetsbibliotek on 05/25/18

constituents Ce, Ru and Sn as shown in Fig. 3. It seems that the broad structure does not arise from a single decay channel. In this stage, the origin of the broad structures was not confirmed experimentally.

3.4 Sm 3d and 4d spectra and the Sm valency in samarium compounds

3.4.1 Separation of Sm^{2+} components from Sm 3d and 4d spectra

As can be seen in Fig. 1, the Sm^{2+} peak due to the final state $3d^94f^6$ was observed at the low binding energy side of the Sm^{3+} peak due to the final state $3d^94f^5$ for $SmRuSn_3$. Whether the presence of the divalent peak is due to initial or final state effects for samarium and its compounds has been continued to discuss.[1,8,10,14] Wertheim and Crecelius[8] have concluded that the presence of the Sm^{2+} peak is due to the initial state effect in the intrinsic surface state for Sm metal.

We measured also the Sm 3*d* and 4*d* XPS spectra of various samarium compounds; Sm metal, $SmAl_2$, $SmGa_2$,[15] SmSb, $SmPd_3$ and Sm_2CuO_4, which are recognized as trivalent samarium compounds. The following materials were also investigated: $Sm_3Rh_4Sn_{13}$ with the same crystal structure as $SmRuSn_3$, SmB_6 known as a mixed valence material, and $SmSn_3$ known as a Kondo alloy.

The XPS spectra of the Sm 3*d* core level are shown in Fig. 4. The general features of these spectra have the same trend as published in literature:[1,4,8-11] it can be seen that the binding energies of the Sm 3*d* levels consisting of the Sm^{3+} and Sm^{2+} peaks are separated by about 10 eV from each other. For $SmPd_3$ and Sm_2CuO_4, the prominent peaks which should appear at the low binding energy side of the Sm^{3+} peaks disappear and the Sm $3d_{5/2}$ peaks show the asymmetric tailing at the low binding energy side.

As can be seen in Fig. 4, the Sm^{2+} peaks appear on the tails of the Sm^{3+} peaks. To estimate the contribution of the Sm^{2+} peak to the Sm 3*d* spectrum, the Sm^{2+} peak was separated from the tailing part of the Sm^{3+} peak. As shown in Fig. 5, the inelastic scattered background indicated by the dashed line was subtracted from the Sm 3*d* spectrum. Next, it was assumed that the Sm^{3+} peak consists of two

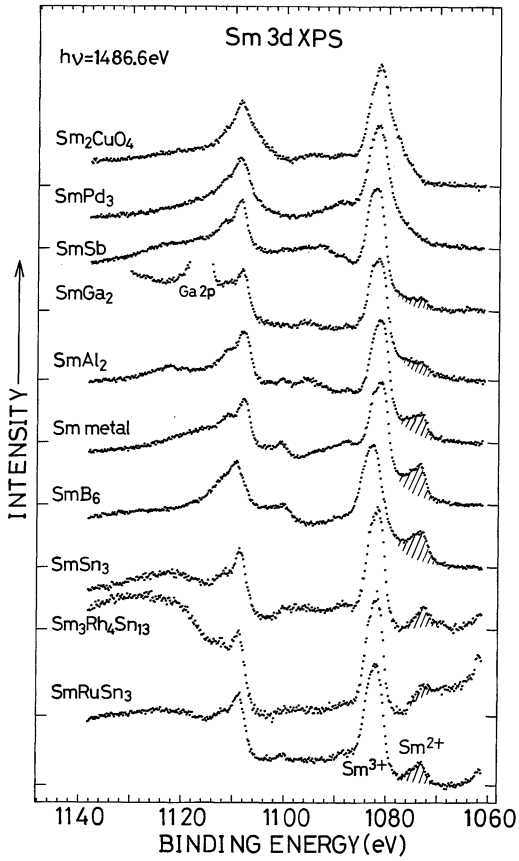

Fig. 4. Sm 3*d* XPS spectra of various samarium compounds. The Sm $3d_{5/2}$ XPS spectra show the Sm^{3+} peaks due to the final state $3d^94f^5$ at the binding energy of ~1082 eV and Sm^{2+} peaks due to the final state $3d^94f^6$ at ~1073 eV. For $SmRuSn_3$, $Sm_3Rh_4Sn_{13}$ and $SmSn_3$, the Sn Auger structures appear at the binding energies of ~1130 eV and ~1060 eV.

components. The Sm^{3+} peak was fitted by the convolution of two Lorentzians with the life time of 2.2 eV and a Gaussian with the width of 1.1 eV. The calculated tailing background of the Sm^{3+} peak was shown by the solid line in the figure. The similar procedures were performed for the other Sm 3*d* XPS spectra.

The Sm 4*d* XPS spectrum is more sensitive to the 4*f* electronic state in the bulk than the Sm 3*d* XPS spectrum because of the difference in mean free path of photoelectrons. The Sm 4*d* XPS spectra of various compounds are shown in Fig. 6. For $SmRuSn_3$, $Sm_3Rh_4Sn_{13}$ and $SmSn_3$, the Sn 4*s* level appeared at the binding energy of about 137 eV. The Sm 4*d*

J. Phys. Soc. Jpn.
Downloaded from journals.jps.jp by Uppsala Universitetsbibliotek on 05/25/18

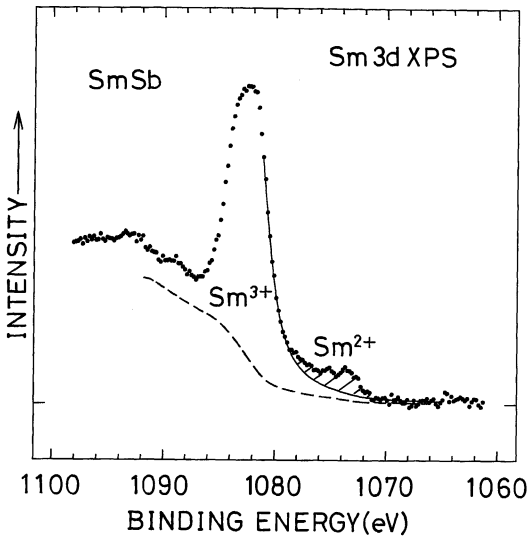

Fig. 5. Sm $3d_{5/2}$ XPS spectrum of a trivalent compound SmSb. The dashed line shows the assumed inelastic scattered background. The solid line indicates the tail of the Sm^{3+} peak obtained by convoluting Lorentzians with a Gaussian.

spectra of these compounds in the figure were obtained by subtracting the Sn 4*s* lines from the observed spectra by use of the intensity ratio of the Sn 4*s* to the Sn 3*d* lines. The Sm^{3+} peaks due to the final state $4d^94f^5$ appear at the binding energies ranging from 125 eV to 145 eV. The Sm^{2+} components[4,16,17] due to the final state $4d^94f^6$ can be seen at the binding energy of about 123 eV except for the spectra of $SmPd_3$ and Sm_2CuO_4.

To estimate the intensity of the Sm^{2+} component in the Sm 4*d* spectrum, the following procedures were performed. As indicated by the dashed line in the spectrum of $SmRuSn_3$ in Fig. 6, the inelastic scattered background was subtracted from the Sm 4*d* spectrum. The similar procedures were performed for the other Sm 4*d* XPS spectra. The Sm 4*d* spectrum of trivalent samarium ions exhibits the complicated multiplet structure due to $4d^94f^5$ configuration. For a divalent samarium compound,[4,16,17] the Sm 4*d* spectrum does not show a complicated multiplet structure compared with the Sm 4*d* spectra of trivalent compounds. For a mixed valence compound SmB_6, the Sm $4d_{5/2}$ component of divalent samarium ions can be separately observed at the binding energy of about 123 eV. From the

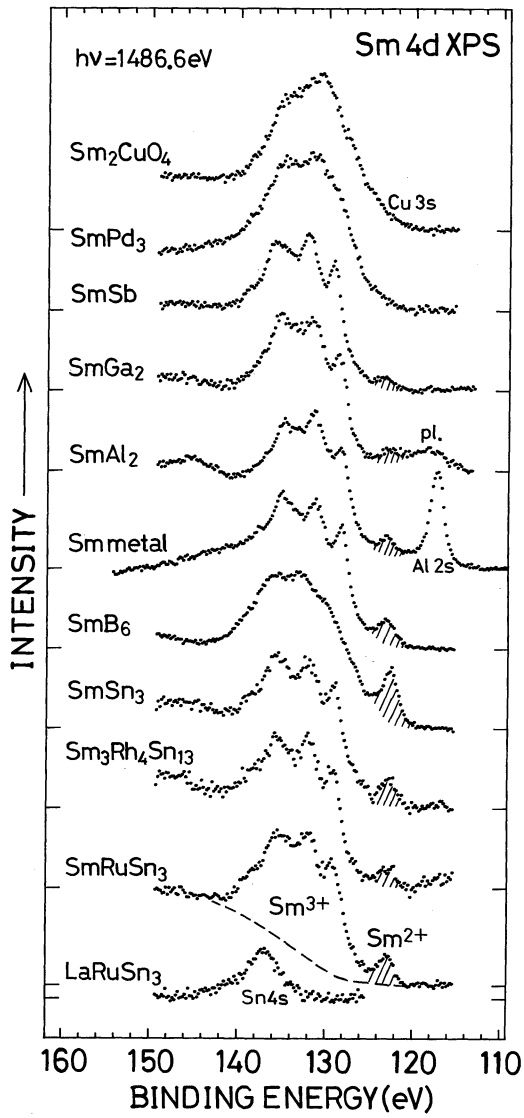

Fig. 6. Sm 4*d* XPS spectra of various samarium compounds and the Sn 4*s* spectrum of $LaRuSn_3$. The Sm 4*d* spectra of $SmRuSn_3$, $Sm_3Rh_4Sn_{13}$ and $SmSn_3$ were obtained by subtracting the Sn 4*s* lines from their respective observed spectra. The complicated structures at the binding energies ranging from ~125 eV to ~145 eV are due to the final state $4d^94f^5$ (Sm^{3+}) and the peaks at ~123 eV are due to the final state $4d^94f^6$ (Sm^{2+}). The dashed line indicates the inelastic background for the Sm 4*d* spectrum of $SmRuSn_3$. The structure (*pl.*) at the binding energy of ~118 eV in the spectrum of $SmGa_2$ is due to the plasmon loss peak accompanying with Ga 3*p* excitation.

experimental results mentioned above, the intensities of the Sm^{2+} peaks were obtained by taking account of the statistical weight of 2:3

J. Phys. Soc. Jpn.
Downloaded from journals.jps.jp by Uppsala Universitetsbibliotek on 05/25/18

for the $4d_{3/2}$ and $4d_{5/2}$ components. The weights of the Sm^{2+} components in the Sm $4d$ spectra were able to be obtained within an experimental error of 0.02 for all the compounds.

3.4.2 *Contribution of the valency of the surface layer to the core-level spectrum*

The weights of the Sm^{2+} peaks in the Sm $4d$ and Sm $3d$ peaks obtained by the procedures described in §3.4.1 are summarized in Fig. 7 for various samarium compounds. For the trivalent samarium compounds, the intensity ratios of the Sm^{2+} peaks in the Sm $4d$ peaks to those in the Sm $3d$ peaks are smaller than the intensity ratios for SmB_6 and $SmRuSn_3$.

To estimate the contribution of the signal from the surface layer to the core-level spectrum quantitatively, the following analysis was given. The fractions of the Sm^{2+} component in the surface layer of thickness of a and that in the bulk are supposed to be α_s and α_b, respectively. The weight of the Sm^{2+} component in the core-level peak (I^{2+}) is given by[8]

$$I^{2+}=\alpha_s\{1-\exp[-a/(\lambda\cos\theta)]\}+\alpha_b\exp[-a/(\lambda\cos\theta)], \quad (1)$$

where θ is the takeoff angle of photoelectrons ejected from a sample and λ is the mean free path of the photoelectron for inelastic scattering. For a trivalent samarium compound, the Sm^{2+} signals are considered to be almost from the surface layer; $\alpha_s \geqq 0$ and $\alpha_b=0$. The contribution of the Sm^{2+} signals from the surface layer to the Sm $3d$ and $4d$ spectra of a trivalent samarium compound was considered on the basis of the following equation,

$$R=\{1-\exp[-a/(\lambda_{4d}\cos\theta)]\}/\{1-\exp[-a/(\lambda_{3d}\cos\theta)]\}. \quad (2)$$

Here R means the intensity ratio of the Sm^{2+} component in the Sm $4d$ peak to that in Sm $3d$ peak, and λ_{4d} and λ_{3d} represent the mean free paths for Sm $4d$ and $3d$ photoelectrons, respectively. The values of R were numerically estimated on the assumption that the thickness of the surface layer is taken as one atomic layer of $a=3$ Å,[8] and that the mean free paths for the photoelectrons are given as $\lambda_{4d}=13\sim18$ Å and $\lambda_{3d}=5\sim10$ Å.[17] The takeoff angle of θ is taken at 45°. The upper and lower limits of the ratios calculated in this way are indicated by two dashed lines in Fig. 7. For a trivalent samarium compound, it can be considered that the measured intensity ratio is to be located in the shaded area between these two dashed lines.

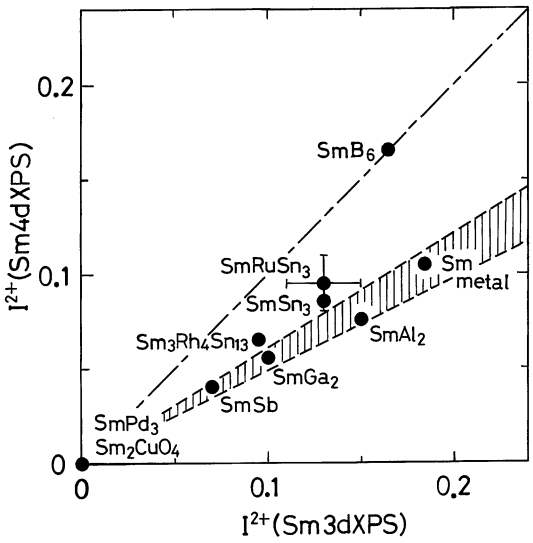

Fig. 7. Relation between the weights of the Sm^{2+} peaks in the Sm $4d$ peaks and those in the Sm $3d$ peaks for various samarium compounds. The weights for the Sm $4d$ XPS spectra are plotted on ordinate and those for the Sm $3d$ XPS spectra on abscissa. The experimental errors of the weights are within 0.02. The experimental errors for $SmRuSn_3$ are typically indicated by the vertical and horizontal bars. When the Sm valency in the surface layer is the same as that in the bulk, the intensity ratio of Sm^{2+} peak in the Sm $4d$ peak to that in the Sm $3d$ peak is plotted on the dash-dotted line.

3.4.3 *Sm valency of $SmRuSn_3$ and its related compounds*

For Sm metal, $SmAl_2$, $SmGa_2$ and SmSb, the intensity ratios of the Sm^{2+} peaks in the Sm $4d$ peaks to those in the Sm $3d$ peaks are plotted in the shaded area in Fig. 7. This indicates that these observed Sm^{2+} signals are from divalent samarium ions in the surface layers. These results are consistent with those for Sm metal by Wertheim and Crecelius[8] and $SmAl_2$ by Raaen and Parks.[10]

For $Sm_3Rh_4Sn_{13}$, we cannot decide within the experimental error whether Sm ions are trivalent in the bulk. The magnetic susceptibility of the sample deviates largely from the theoretical susceptibility of Van Vleck-Frank

J. Phys. Soc. Jpn.
Downloaded from journals.jps.jp by Uppsala Universitetsbibliotek on 05/25/18

Sm^{3+} at temperatures below 100 K.

For a Kondo alloy $SmSn_3$, the presence of divalent samarium ions in the bulk may be possible.

For $SmRuSn_3$, it is concluded that the Sm^{2+} peaks observed in both the Sm $3d$ and Sm $4d$ XPS spectra are attributed to the presence of divalent samarium ions in both the surface layer and bulk; $SmRuSn_3$ is classified under the category of a mixed valence system. To see the dependence of the weight of the Sm^{2+} peak in the core level on the mean free path of photoelectrons furthermore, the Sm $3d$ XPS spectrum was measured using Mg $K\alpha$ radiation. At this excitation, the kinetic energy of the photoelectrons excited from the Sm $3d$ level is about 175 eV and the mean free path is about 4 Å.[17] The weight of the Sm^{2+} peak in the Sm $3d$ peak was estimated to be about 0.18. The Sm valency in $SmRuSn_3$ is estimated to be 2.95 ± 0.02 in the bulk and to be 2.75 ± 0.05 in the surface layer by use of eq. (1).

§4. Conclusions

We measured the core-level XPS spectra of $RERuSn_3$ (RE=La, Ce, Pr, Nd and Sm) and their related compounds. The two conclusions from these measurements are as follows.

(1) The Ce $3d$ XPS spectra of $CeRuSn_x$ (x=2.85, 3.0 and 3.15) show the absence of f^0 structure and the weak intensity of f^2 peak. These features are similar to those of other heavy fermion compounds. The change of the spectral shape with Sn content x could not be observed within the experimental accuracy.

(2) The core-level XPS spectra of $SmRuSn_3$ show the two-peaked structure consisting of Sm^{2+} and Sm^{3+} peaks. The contribution of the signals from divalent samarium in the surface layer to the core-level spectra was considered by the measurement of the Sm $3d$ and $4d$ XPS spectra of trivalent samarium compounds Sm metal, $SmAl_2$, $SmGa_2$, SmSb, $SmPd_3$ and Sm_2CuO_4. It was found that the intensity ratio of the Sm^{2+} peak in the Sm $4d$ peak to that in the Sm $3d$ peak for $SmRuSn_3$ is larger than the ratios for these trivalent samarium compounds. This indicates that $SmRuSn_3$ is a mixed valence system. The Sm valency in $SmRuSn_3$ was estimated to be 2.95 ± 0.02 in the bulk and 2.75 ± 0.05 in the surface layer.

References

1) F. U. Hillebrecht and J. C. Fuggle: Phys. Rev. B**25** (1982) 3550.
2) J. C. Fuggle, F. U. Hillebrecht, Z. Zolnierek, R. Lässer, Ch. Freiburg, O. Gunnarsson and K. Schönhammer: Phys. Rev. B**27** (1983) 7330.
3) L. Schlapbach, S. Hüfner and T. Riesterer: J. Phys. C**19** (Solid Stat. Phys.) (1986) L63.
4) M. Campagna, G. K. Wertheim and Y. Baer: *Photoemission in Solids II*, ed. L. Ley and M. Cardona (Springer-Verlag, Berlin, Heidelberg and New York, 1979) p. 217.
5) O. Gunnarsson and K. Schönhammer: Phys. Rev. B**28** (1983) 4315.
6) A. Kotani: *Core-Level Spectroscopy in Condensed Systems*, ed. J. Kanamori and A. Kotani (Springer-Verlag, Berlin, Heidelberg, New York, London, Paris and Tokyo, 1987) p. 3.
7) T. Fukuhara, I. Sakamoto and H. Sato: J. Phys. Condens. Matter **3** (1991) 8917.
8) G. K. Wertheim and G. Crecelius: Phys. Rev. Lett. **40** (1978) 813.
9) G. K. Wertheim: J. Electron Spctrosc. Relat. Phenom. **15** (1979) 5.
10) S. Raaen and R. D. Parks: Phys. Rev. B**27** (1983) 6469.
11) G.Krill, J. P. Senateur and A. Amamou: J. Phys. F**10** (Metal Phys.) (1980) 1889.
12) H. Arai, S. Nakai, T. Mituishi, T. Suzuki, H. Ishii and H. Maezawa: preprint.
13) M. Takeshige, O. Sakai and T. Kasuya: J. Phys. Soc. Jpn. **60** (1991) 666.
14) J. N. Andersen, I. Chorkendorff, J. Onsgaard, J. Ghijsen, R. L. Johnson and F. Grey: Phys. Rev. B**37** (1988) 4809.
15) I. Sakamoto, T. Miura, K. Miyoshi and H. Sato: Physica B**165** & **166** (1990) 339.
16) J.-N. Chazalviel, M. Campagna, G. K. Wertheim and P. H. Schmidt: Phys. Rev. B**14** (1976) 4586.
17) D. A. Shirley: *Photoemission in Solids I*, ed. L. Ley and M. Cardona (Springer-Verlag, Berlin, Heidelberg and New York, 1979) p. 165.